High-Resolution Time-Frequency Representations Based on the Local Polynomial Fourier Transform for Over-the-Horizon Radars

Igor Djurović[a], Slobodan Djukanović*[a], Moeness G. Amin[b], Yimin D. Zhang[b], and Braham Himed[c]

[a]Electrical Engineering Department, University of Montenegro, Cetinjski put bb, 81000 Podgorica, Montenegro;
[b]Center for Advanced Communications, Villanova University, Villanova, PA 19085, USA;
[c]Air Force Research Laboratory, AFRL/RYMD, Dayton, OH 45433, USA

ABSTRACT

In this paper, we consider resolving over-the-horizon radar (OTHR) Doppler returns. A high-resolution time-frequency (TF) representation of the received signal is obtained by using the local polynomial Fourier transform (LPFT). From the optimally concentrated LPFT, multicomponent Doppler signatures, which are only several frequency bins apart, are extracted using an instantaneous frequency estimation method based on the Viterbi algorithm. The performance of the proposed method is validated using real data.

Keywords: Over-the-horizon radar, instantaneous frequency estimation, Viterbi algorithm, local-polynomial Fourier transform.

1. INTRODUCTION

Over-the-horizon radar (OTHR) performs wide-area surveillance at ranges well beyond the limit of conventional line-of-sight (LOS) radars.[1] Maneuvering targets generate multi-component Doppler signatures corresponding to the direct and non-direct paths, both encounter reflections from the ionosphere. These signatures contain important information about the position, maneuvering and altitude of the targets, and they are usually characterized by significant variation of their instantaneous frequencies (IFs). If properly estimated, the multi-component target Doppler signatures reveal the moving target altitude trajectories. Time-frequency (TF) methods can be successfully applied for high-resolution analysis of the OTHR Doppler returns.[2] Clearly, the main challenge facing parametric and nonparametric time-frequency representation methods in OTHR is the ability to resolve close signal components arising from close Doppler values when the aircraft is viewed by different multipaths. It is noted that in the TF plane, the Doppler components can be only several frequency bins apart and even visual detection could be hardly done. High-resolution methods, such as the Capon and the MUSIC techniques, cannot be applied due to the IF variations. The use of bilinear TF signal representations, either in non-adaptive or adaptive mode, is also restricted due to inherent interferences. The spectrogram, as a very popular TF tool, has poor resolution for such OTHR Doppler signals.

In this paper, we propose a hybrid TF-based method for resolving OTHR Doppler returns. The method comprises several recently proposed tools and its high-quality performance is validated using real data. First, the Viterbi algorithm-based IF estimator[3] is used to detect the TF-domain positions of the signal of interest in heavily cluttered data. After detecting regions of interest, the local polynomial Fourier transform (LPFT) is used to produce high-resolution TF representations without cross-terms.[4] In the LPFT, the adaptive chirp-rate is estimated at each time instant and selected to compensate higher order terms in the signal's IF and, as such, improve the signal concentration. Finally, an efficient high-resolution interpolation strategy is used to refine the estimation of the considered signal component.

The paper is organized as follows. In Section 2, background material regarding signal model, Doppler characteristics of the received signal, the LPFT and the IF estimation based on the Viterbi algorithm is presented. The proposed method is introduced and validated in Section 3. Section 4 concludes the paper.

*slobdj@ac.me; phone +382 20 245-839; fax +382 20 245-873; www.tfsa.me

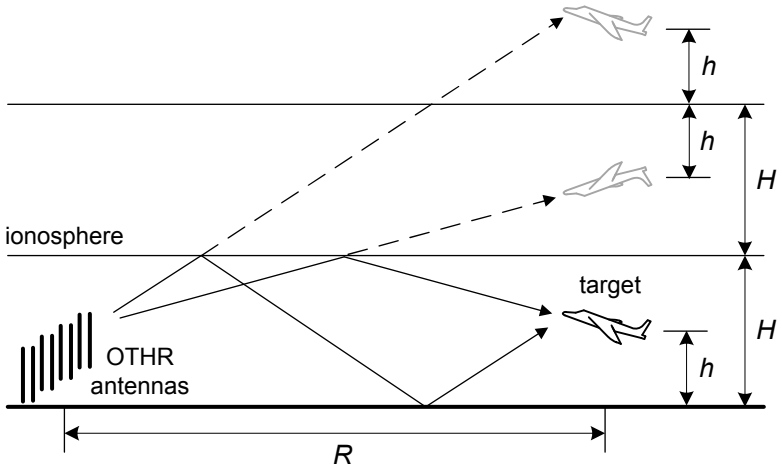

Figure 1. Flat ground model of the OTHR system.

2. BACKGROUND

2.1 Signal model and Doppler characteristics

In this paper, we will adopt the flat ground model of the OTHR system for the simplicity of mathematical analysis. The model is presented in Fig. 1. After pulse or sweep matched filtering and beamforming at the receiver side, the received signal $y(t)$ can be expressed as

$$y(t) = x(t) + u(t) + n(t), \tag{1}$$

where $x(t)$ represents the return signal from the target, $u(t)$ the clutter, and $n(t)$ the ambient noise. Signal $x(t)$ can be expressed as

$$x(t) = Ae^{-j\omega_c(d_t+d_r)/c}, \tag{2}$$

where A is a complex scalar that represents the propagation loss and phase, d_t and d_r are the one-way slant range between the transmitter and the target, and between the target and the receiver, respectively, c is the speed of light and $\omega_c = 2\pi f_c$ is the carrier frequency. In this paper, the noise term $n(t)$ is ignored, since its power is usually very small compared to the other components of the received signal. Typically, in the OTHR system, two paths of the radar signal exist, one directly reflected from the ionosphere, and the other reflected from the earth surface (ocean or ground) near the target, as shown in Fig. 1. The propagation distance of the two paths will be denoted as l_1 and l_2, respectively. Therefore, if we assume that the OTHR system is a monostatic one (location of the transmitter and receiver coincide), d_t and d_r can take the value of either l_1 and l_2. If we denote the path losses corresponding to l_1 and l_2 as A_1 and A_2, respectively, the radar return will contain four components corresponding to four combination paths: $(l_1 : l_1)$ as path I, $(l_2 : l_2)$ as path II, and combination of paths $(l_1 : l_2)$ and $(l_2 : l_1)$ as path III. The radar return can be now expressed as

$$x(t) = A_1e^{-j\omega_c 2l_1/c} + A_2e^{-j\omega_c 2l_2/c} + A_3e^{-j\omega_c(l_1+l_2)/c}. \tag{3}$$

From Fig. 1, the distances l_1 and l_2 can be expressed in terms of the range distance R, the ionosphere height H and the aircraft height h, as follows:

$$\begin{aligned} l_1 &= \sqrt{R^2 + (2H-h)^2} \approx R + \frac{2H^2 - 2Hh}{R}, \\ l_2 &= \sqrt{R^2 + (2H+h)^2} \approx R + \frac{2H^2 + 2Hh}{R}. \end{aligned} \tag{4}$$

The approximations in (4) are derived having in mind that, in a typical OTHR scenario, we can assume that $R \gg H \gg h$.

Generally, the flight of an aircraft consists of horizontal and elevation movements. Herein, we consider the Doppler frequency characteristics of the aircrafts movement in the two different dimensions.

As an aircraft flies, R, and possibly also h, become functions of t. The height of the ionosphere H is also slowly time-varying. However, we assume that H is constant over the processing time interval. From (4), we have

$$\begin{aligned} \frac{dl_1(t)}{dt} &\approx K(t)v_R(t) - \frac{2H}{R(t)}v_c(t), \\ \frac{dl_2(t)}{dt} &\approx K(t)v_R(t) + \frac{2H}{R(t)}v_c(t), \end{aligned} \tag{5}$$

where

$$\begin{aligned} K(t) &= 1 - 2H^2/R^2(t), \\ v_R(t) &= dR(t)/dt, \\ v_c(t) &= dh(t)/dt. \end{aligned} \tag{6}$$

In (6), $v_R(t)$ and $v_c(t)$ are the target velocity in the range direction toward the radar and the ascending velocity of the target, respectively. The Doppler frequencies corresponding to the three different paths are obtained as

$$\begin{aligned} f_{\mathrm{I}}(t) &= \frac{2f_c}{c}\frac{dl_1(t)}{dt} \approx \frac{2f_c}{c}K(t)v_R(t) - \frac{4f_cH}{R(t)c}v_c(t), \\ f_{\mathrm{II}}(t) &= \frac{2f_c}{c}\frac{dl_2(t)}{dt} \approx \frac{2f_c}{c}K(t)v_R(t) + \frac{4f_cH}{R(t)c}v_c(t), \\ f_{\mathrm{III}}(t) &= \frac{f_c}{c}\frac{dl_1(t)+dl_2(t)}{dt} \approx \frac{2f_c}{c}K(t)v_R(t). \end{aligned} \tag{7}$$

From (7), the information about the aircraft height $h(t)$ can be obtained by integrating the difference between the Doppler frequencies.

If the target is changing its acceleration, height or direction, the velocity v_R becomes time-varying and the standard DFT-based approach does not provide high Doppler resolution even with a long coherent integration time (CIT).[5] In this case, the detection and estimation of the Doppler shift caused by a change of h become difficult. The presence of strong clutter introduces additional difficulties. Due to low resolution, the spectrogram and related TF-based methods smear the time-Doppler signatures of the target and therefore cannot be used to resolve them.[2] On the other hand, high-resolution Wigner distribution produces undesirable cross-terms when multicomponent signals are considered, which can completely cover the target's signatures in the TF plane.

2.2 Local polynomial Fourier transform

The LPFT has been introduced in the TF analysis in,[6] and the M-th order LPFT is defined as

$$\mathrm{LPFT}(t,\omega;\vec{\omega}) = \int_{-\infty}^{\infty} x(t+\tau)w(\tau)e^{-j\theta(\vec{\omega},\tau)}e^{-j\omega\tau}d\tau, \tag{8}$$

where

$$\theta(\vec{\omega},\tau) = \omega_1\frac{\tau^2}{2!} + \omega_2\frac{\tau^3}{3!} + \cdots + \omega_M\frac{\tau^{M+1}}{(M+1)!} \tag{9}$$

is a polynomial of order $(M+1)$ with variable τ, and $\vec{\omega} = (\omega_1, \omega_2, \cdots, \omega_M)$ is the polynomial coefficients vector. According to (8), the LPFT represents the Fourier transform (FT) of the product of signal, window and exponential of polynomial, i.e.

$$\mathrm{LPFT}(t,\omega;\vec{\omega}) = \mathrm{FT}\left[x(t+\tau)\,w(\tau)\,e^{-j\theta(\vec{\omega},\tau)}\right], \tag{10}$$

where FT[·] represents the FT operator.

The LPFT is an $(m+1)$ dimensional transform which concentrates at

$$\vec{\omega} = (\phi^{(1)}(t), \phi^{(2)}(t), ..., \phi^{(m)}(t)), \tag{11}$$

where $\phi(t)$ is the signal's phase, and $\phi^{(i)}(t)$, $i = 2, 3, \cdots, m+1$, is the i-th phase derivative.[6] Definition (8) also implies that the short-time Fourier transform (STFT) represents a special case of the LPFT obtained when $\vec{\omega}$ is a zero-vector. Similarly to the STFT, the LPFT is a linear transform that does not produce cross-terms when $x(t)$ is a multicomponent signal.[6]

Specially, the first-order LPFT,

$$\text{LPFT}(t, \omega; \omega_1) = \int_{-\infty}^{\infty} x(t+\tau) w(\tau) e^{-j\omega_1 \frac{\tau^2}{2}} e^{-j\omega\tau} d\tau \tag{12}$$

of a linear FM signal

$$x(t) = e^{j\left(at + b\frac{t^2}{2}\right)} \tag{13}$$

equals

$$\text{LPFT}(t, \omega; \omega_1) = e^{j\left(at + b\frac{t^2}{2}\right)} \int_{-\infty}^{\infty} w(\tau) e^{-j(\omega - a - bt)\tau} e^{-j(\omega_1 - b)\frac{\tau^2}{2}} d\tau. \tag{14}$$

For $\omega_1 = b$, the quadratic variation of the phase is compensated within the considered window, so the first-order LPFT reduces to the STFT of a sinusoid with frequency $a + bt$ and initial phase $at + b\frac{t^2}{2}$. Analytically,

$$\text{LPFT}(t, \omega; \omega_1) = e^{j\left(at + b\frac{t^2}{2}\right)} \int_{-\infty}^{\infty} w(\tau) e^{-j(\omega - a - bt)\tau} d\tau = e^{j\left(at + b\frac{t^2}{2}\right)} W(\omega - a - bt), \tag{15}$$

where $W(\omega)$ represents the FT of window $w(\tau)$.

The discrete form of the LPFT is defined as follows:

$$\begin{aligned} \text{LPFT}(n, k) &= \sum_{m=-\frac{N}{2}}^{\frac{N}{2}-1} x(n+m) w(m) e^{-j\sum_{i=1}^{M} \omega_i \frac{m^{i+1}}{(i+1)!}} e^{-j\frac{2\pi}{N}mk} \\ &= \text{DFT}\left[x(n+m)\, w(m)\, e^{-j\sum_{i=1}^{M} \omega_i \frac{m^{i+1}}{(i+1)!}} \right] \end{aligned} \tag{16}$$

where $x(n)$ and $w(m)$ are discrete versions of signal and window, respectively, and DFT$[\cdot]$ represents the discrete FT operator.

In Fig. 2, we compare the STFT and the LPFT for two FM types of signals, namely linear FM and sinusoidal FM signal. The signal length is 512 and the Hanning window of length 128 is used in calculation of both the STFT and LPFT. In the case of linear FM signal (top row in Fig. 2), the first-order LPFT, denoted as LPFT^1, is considered and it is calculated for the optimal coefficient value in accordance with (15). The bottom row in Fig. 2 represents results obtained for the sinusoidal FM signal. Now, the second-order LPFT, denoted as LPFT^2, is considered and its coefficients ω_1 and ω_2 are calculated according to (11), i.e., ω_1 and ω_2 correspond to the second-order and third-order phase derivative, respectively, calculated at the central window position. Although higher order phase derivatives exist, in this case only the first two terms suffice to properly concentrate the signal in the TF plane.

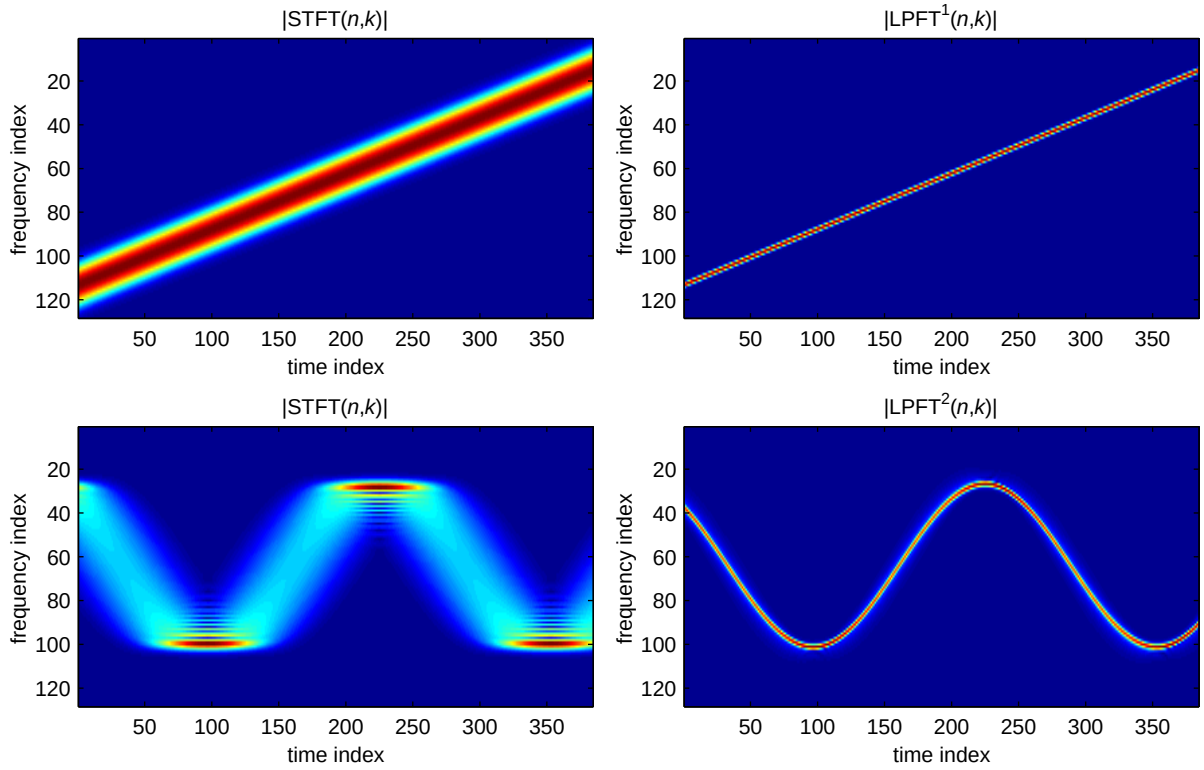

Figure 2. *Top row:* The STFT and the first-order LPFT of a linear FM signal. *Bottom row:* The STFT and the second-order LPFT of a sinusoidal FM signal.

2.3 IF estimation based on the Viterbi algorithm

The IF estimation algorithm used in this paper is proposed in[3] and is based on the edge-following algorithm in digital image processing proposed in.[7] The problem in[7] was to find a line that passes through pixels with as high as possible values of the edge detector, and such that variations of the edge direction are as small as possible. Our estimation algorithm may be viewed as connecting points on a map such that the path length and the altitude variations are as small as possible. The problem can be resolved in a recursive manner using the well known Viterbi algorithm.[8]

Let us consider the time interval $n \in [n_1, n_2]$, and assume that all paths between n_1 and n_2 belong to a set $\mathbf{K}$ and that these paths can take only discrete frequency values belonging to a set Q_k.

The IF estimation is obtained as

$$\begin{aligned}\hat{\omega}(n) &= \underset{K(n)\in\mathbf{K}}{\arg\min}\left[\sum_{n=n_1}^{n_2-1} g(K(n),K(n+1)) + \sum_{n=n_1}^{n_2} f(\mathrm{TF}(n,K(n)))\right] \\ &= \underset{K(n)\in\mathbf{K}}{\arg\min}\, p(K(n);n_1,n_2),\end{aligned} \tag{17}$$

where $p(K(n);n_1,n_2)$ is the sum of penalty functions $g(x,y)$ and $f(x)$, along the line $K(n)$, from the instant n_1 to n_2, and $\mathrm{TF}(n,k)$ represents a TF transform of the considered signal. Function $g(x,y) = g(|x-y|)$ is a nondecreasing one with respect to $|x-y|$ (between the IF values in the consecutive points $x = K(n)$ and $y = K(n+1)$), while $f(x)$ is a nonincreasing function of $x = \mathrm{TF}(n,K(n))$. In this way, larger values of $\mathrm{TF}(n,K(n))$ are more important candidates for the IF estimation at the considered instant. For the considered n, $f(x)$ can be formed as follows. The values of $\mathrm{TF}(n,k)$, $k \in Q_k$, are sorted into the nonincreasing order, i.e.

$$\mathrm{TF}(n,k_1) \geq \mathrm{TF}(n,k_2) \geq \cdots \geq \mathrm{TF}(n,k_M), k_j \in Q_k, j \in [1,M], \tag{18}$$

where $j = 1, 2, ..., M$, is the position within the sorted sequence. Then, the function $f(x)$ is formed as

$$f(\mathrm{TF}(n, k_j)) = j - 1, \tag{19}$$

which corresponds to the idea that larger transform values yield smaller $f(x)$ values and therefore are more important candidates for the IF estimates.

For a constant $g(x, y)$, the IF estimation (17) is reduced to finding the position of the transform maxima, i.e., the function $f(x)$ completely determines the minimum of (17). In this paper, we will use a linear form of $g(x, y)$ for the difference between two points greater than an assumed threshold Δ[3]

$$g(x,y) = \begin{cases} 0 & |x-y| \leq \Delta \\ c(|x-y| - \Delta) & |x-y| > \Delta. \end{cases} \tag{20}$$

The reasonable choice for Δ would be the maximal expected value of the IF variation between consecutive points. It means that there is no additional penalty due to this function for small IF variation (within Δ points, for two consecutive instants). In the realization we obtained good results by taking Δ which corresponds to a few neighboring points (for example, values around $\Delta = 3$). For $\Delta \to \infty$, the estimation given by (17) will reduce to the estimation based on the transform maxima.

The optimization problem (17) will be solved as follows. Let the TF plane contain M frequencies and Q time-instants, $\mathbf{T} = \{(n_i, k_j) | i \in [1, Q], j = [1, M]\}$. The total number of paths between two ending points is M^Q. This fact makes a direct search for the optimal path impossible. Fortunately the algorithm can be realized recursively, as an instance of the generalized Viterbi algorithm.[8] Its realization can be described by the following fundamental steps.

(a) Let optimal paths, which connect the instant n_1 and all points to the instant n_i, are determined. These paths, denoted as $\pi_i(n; k_j)$, $n \in [n_1, n_i]$ for $j \in [1, M]$ can be written as

$$\pi_i(n; k_j) = \underset{K(n) \in \mathbf{K}_{ij}}{\arg\min}\, p(K(n); n_1, (n_i, k_j)), \quad j \in [1, M], \tag{21}$$

where the set $\mathbf{K}_{ij}$ contains all the paths between the instant n_1 and the point (n_i, k_j), while $p(K(n); n_1, (n_i, k_j))$ is the sum of the path penalty functions for the line $K(n)$. In the Viterbi algorithm terminology, paths (21) are known as the *partial best paths*. Current IF estimate, within the interval $[n_1, n_i]$, can be written as:

$$\hat{\omega}_{(i)}(n) = \underset{\pi_i(n;k_j), j \in [1,M]}{\arg\min}\, p(\pi_i(n; k_j); n_1, (n_i, k_j)), \tag{22}$$

for the interval $[n_1, n_i]$.

(b) The partial best paths at the next instant n_{i+1} can be represented as concatenation of (21) with the points at the new instant $\pi_{i+1}(n; k_j) = [\pi_i(n; k_l), (n_{i+1}, k_j)]$, $j \in [1, M]$, for $l \in [1, M]$, that produce the minimal value of

$$p(\pi_i(n; k_l); n_1, (n_i, k_l)) + g(k_l, k_j) + f(\mathrm{TF}(n_{i+1}, k_j)), \tag{23}$$

for each k_j, $j \in [1, M]$. Note that the function $f(\mathrm{TF}(n_{i+1}, k_j))$ is constant for the considered partial best path. Generally, for the considered point it is necessary to search over M paths, M^2 for the entire instant, and QM^2 for the entire plane.

Step (b) should be repeated for each point.

In,[3] the described IF estimation algorithm is illustrated in detail using an example of a TF plane with $M = 3$ and $Q = 8$ points. For additional applications of the Viterbi algorithm we refer to.[9,10]

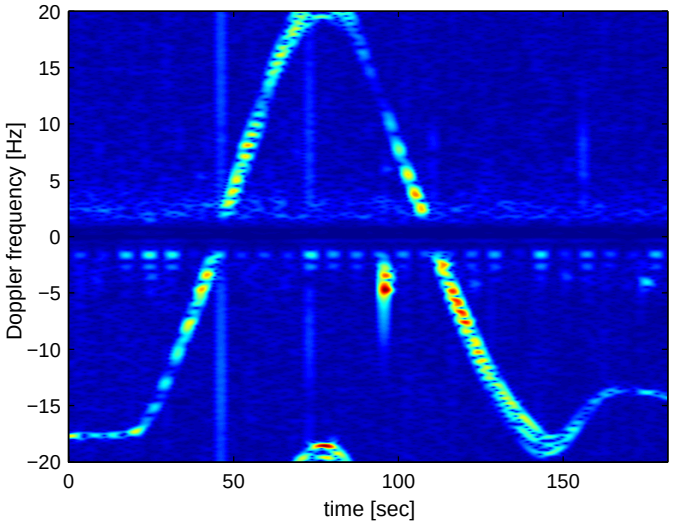

Figure 3. The spectrogram of the received signal.

3. HIGH-RESOLUTION METHOD FOR TARGET DETECTION IN THE OTHR

In this section, we propose a high-resolution method for target detection and classification in the OTHR. As a TF tool, the method uses the LPFT. By adopting shorter analysis window, we can use the first-order LPFT to successfully resolve components of the received signal in the TF plane. We also assume that the clutter has been suppressed.[2]

The proposed method can be described by the following steps:

Step 1. Detecting TF region of interest In this step, we detect the TF region where time-Doppler frequency signatures are located. To that end, we apply the IF estimation based on the Viterbi algorithm on the spectrogram of the received signal. We do not consider signature separation at this point.

Step 2. Optimizing LPFT in detected TF region of interest After the TF region containing time-Doppler frequency signatures is detected, we optimize the LPFT within that region. The optimal LPFT is one with the most concentrated signatures. We assume that all the three signatures are parallel so that the optimal concentration of one signature implies the optimal concentration of other signatures.

Step 3. Extracting signatures Time-Doppler frequency signatures are extracted from the optimal LPFT. The IF of the strongest signature is estimated by applying the Viterbi algorithm-based IF estimation on the optimal LPFT. After the IF is estimated, the obtained signature is removed by excising a band of frequencies around the obtained signature. The procedure is repeated two more times to obtain the other two time-Doppler frequency signatures.

The proposed method is evaluated on real data.[11] The duration of the received signal, sampled at $F_s = 40$Hz, is 181.6 sec. In the received signal, the clutter has been suppressed. The spectrogram of the received signal is represented in Fig. 3. It is calculated using the Hanning window with 256 samples. Time-Doppler signatures in the spectrogram are completely obscured. Although the spectrogram cannot be used for signature resolving, it can be used in our method to detect the TF region where signatures are located. Clearly, the IF estimation based on the maxima of the spectrogram would not yield satisfactory results. Therefore, we use the IF estimation based on the Viterbi algorithm. The obtained IF estimation is depicted by the thick solid line in Fig. 4, whereas the TF region of interest is delimited by the dotted lines. Note that the IF estimation algorithm successfully deals with a strong remaining clutter that occurs at around 95 sec and -5 Hz, even though the spectrogram maximum corresponds to this clutter component. In general, the Viterbi algorithm can successfully extract IF trajectories containing many discontinuities, which is not the case for the maxima based estimation.

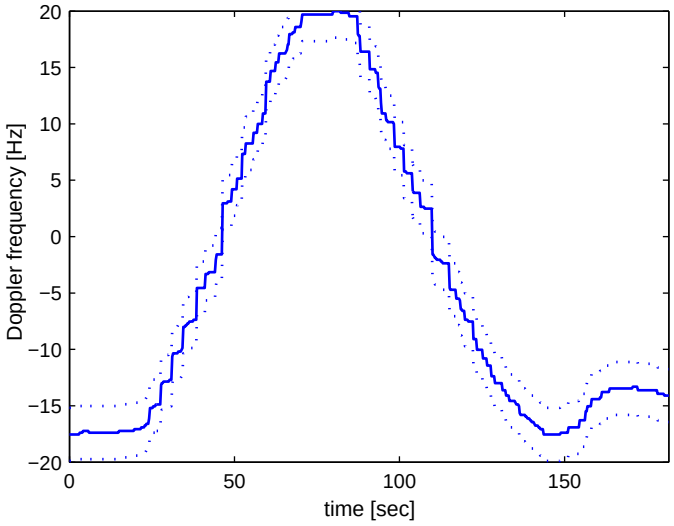

Figure 4. The IF estimation obtained from the spectrogram of the received signal (see Fig. 3). The solid line represents the IF estimation, while the dotted lines delimit the TF region of interest.

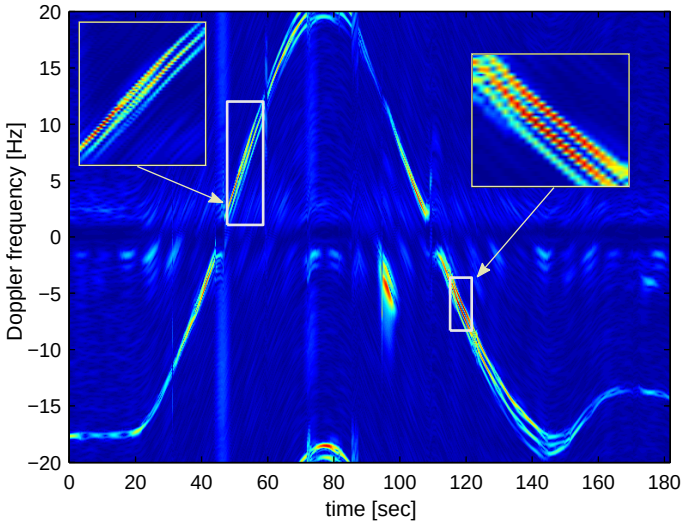

Figure 5. The optimal first-order LPFT of the received signal.

After obtaining the TF region of interest, we perform the LPFT optimization of signatures within that region. In this paper, we consider the first-order LPFT, i.e., we approximate the signatures within the considered window as linear FM signals. In order to optimize the first-order LPFT, we first adopt a finite set Ω_1 of coefficients ω_1 and, for each time instant n, we calculate the LPFT for all values of ω_1 from Ω_1. The optimal LPFT is one with the best concentration in the TF plane, where we use the concentration measure introduced in[12] obtained as the ratio of the L_4 norm to the square of the L_2 norm of the LPFT, i.e., the optimal ω_1 at time instant n, denoted as $\omega_1^{\text{opt}}(n)$, is obtained as

$$\omega_1^{\text{opt}}(n) = \arg\min_{\omega_1 \in \Omega_1} \frac{\sum_k |\text{LPFT}(n,k)|^4}{\left(\sum_k |\text{LPFT}(n,k)|^2\right)^2}. \tag{24}$$

The optimal first-order LPFT of the underlying signal is presented in Fig. 5. Now the presence of three close time-Doppler frequency signatures is obvious during a significant part of signal length. Two TF regions in Fig. 5 are zoomed to emphasize the presence of three signatures. In addition, the signatures are parallel, implying that all the three signatures are optimized simultaneously.

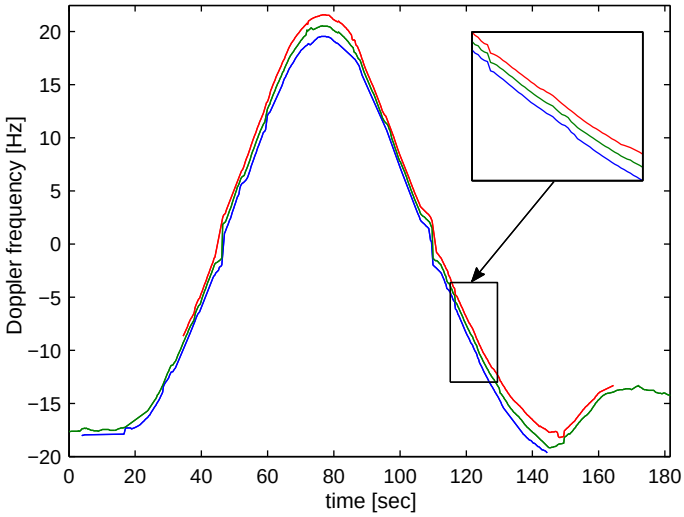

Figure 6. The extracted time-Doppler frequency signatures from the LPFT of the received signal.

In order to extract the signatures from the optimal LPFT, we perform the Viterbi algorithm-based IF estimation three times, once for each signature. We start with the strongest signature. After its IF is estimated, we remove it by excising a narrow TF band around the obtained IF estimation. The procedure is repeated for the next strongest signature, and finally for the weakest signature. Since the signatures are close to each other and have similar amplitudes, it may happen that the Viterbi algorithm "jumps" from one signature to another. Therefore, to obtain the final smooth signatures we perform two steps. The first one is to sort the obtained estimates in frequency at each time instant. In the second step, we form three signatures, namely top, middle and the bottom one, by connecting estimates with the highest, middle and lowest frequency, respectively. The final signatures are depicted in Fig. 6. Note that the spectrum aliasing, that occurs around 75 sec, has been corrected in the IF estimation.

A closer look at Fig. 6 reveals that the proposed algorithm has not extracted all the three signatures within some time intervals. By observing the LPFT in Fig. 5, we see that the signatures overlap within some time intervals so that they cannot be distinguished. Furthermore, in order to suppress the occurrence of false signatures, we performed amplitude thresholding in the signature extraction procedure by discarding all the signature candidates whose amplitude is below 3% of the maximum of the LPFT within the TF region of interest.

4. CONCLUSIONS

We proposed a TF-based method for resolving OTHR Doppler returns. As a TF tool, the LPFT is used and it is shown that it can successfully resolve close non-stationary time-Doppler frequency signatures. The IF estimation is performed using the Viterbi algorithm-based approach that can deal with the IF signatures containing many discontinuities. Simulations carried out on the real data prove the robustness and effectiveness of the proposed method.

ACKNOWLEDGMENT

The work of I. Djurović is supported in part by the Ministry of Science of Montenegro and the Montenegrin Academy of Sciences and Arts. The work of S. Djukanović is supported in part by the Ministry of Science of Montenegro. The work of Y. D. Zhang and M. G. Amin is supported in part by a subcontract with Dynetics, Inc. for research sponsored by the Air Force Research Laboratory (AFRL) under Contract FA8650-08-D-1303. The authors would like to thank Dr. Gordon Frazer of the Australian Defence Science and Technology Organisation for providing the real measurement data used in this paper.

REFERENCES

[1] Headrick, J. and Skolnik, M., "Over-the-horizon radar in the HF band," *Proceedings of the IEEE* **62**, 664–673 (June 1974).

[2] Zhang, Y., Amin, M., and Frazer, G., "High-resolution time-frequency distributions for manoeuvring target detection in over-the-horizon radars," *Radar, Sonar and Navigation, IEE Proceedings* - **150**, 299–304 (August 2003).

[3] Djurović, I. and Stanković, LJ., "An algorithm for the Wigner distribution based instantaneous frequency estimation in a high noise environment," *Signal Processing* **84**, 631–643 (March 2004).

[4] Djurović, I., Thayaparan, T., and Stanković, LJ., "Adaptive local polynomial fourier transform in ISAR," *EURASIP J. Appl. Signal Process.* **2006**, 1–15 (January 2006).

[5] Wang, G., Xia, X.-G., Root, B., Chen, V., Zhang, Y., and Amin, M., "Manoeuvring target detection in over-the-horizon radar using adaptive clutter rejection and adaptive chirplet transform," *Radar, Sonar and Navigation, IEE Proceedings* - **150**, 292–298 (August 2003).

[6] Katkovnik, V., "A new form of the Fourier transform for time-varying frequency estimation," *Signal Processing* **47**, 187–200 (November 1995).

[7] Martelli, A., "Edge detection using heuristic search methods," *Computer Graphics and Image Processing* **1**, 169–182 (August 1972).

[8] Forney, G.D., "The Viterbi algorithm," *Proceedings of the IEEE* **61**, 268–278 (March 1973).

[9] Conru, C., Djurovic, I., Ioana, C., Quinquis, A., and Stankovic, L., "Time-frequency detection using Gabor filter bank and Viterbi based grouping algorithm," in [*Acoustics, Speech, and Signal Processing, 2005. Proceedings. (ICASSP '05). IEEE International Conference on*], (March 2005).

[10] Stankovic, LJ., Djurovic, I., Ohsumi, A., and Ijima, H., "Instantaneous frequency estimation by using Wigner distribution and Viterbi algorithm," in [*Acoustics, Speech, and Signal Processing, 2003. Proceedings. (ICASSP '03). 2003 IEEE International Conference on*], **6** (April 2003).

[11] Ioana, C., Zhang, Y., Amin, M., Ahmad, F., Frazer, G., and Himed, B., "Time-frequency characterization of micro-multipath signals in over-the-horizon radar," in [*IEEE Radar Conference, Atlanta, GA*], (May 2012).

[12] Jones, D. and Parks, T., "A high resolution data-adaptive time-frequency representation," *Acoustics, Speech and Signal Processing, IEEE Transactions on* **38**, 2127–2135 (December 1990).